Progress In Electromagnetics Research, PIER 12, 75–105, 1996

MODELING MULTIPLE INTERACTING SMALL APERTURES FOR EMI APPLICATIONS USING THE FINITE-DIFFERENCE TIME-DOMAIN TECHNIQUE

J. H. Oates, R. T. Shin, M. J. Tsuk

1. Introduction

The modeling of small apertures for Electromagnetic Interference (EMI) applications using the Finite-Difference Time-Domain (FDTD) technique has recently been presented [1]. That paper addressed the problem of an isolated small aperture. However, in typical applications it is an array of closely spaced apertures which is of interest, such as is used, for example, for cooling of computers and other electronic equipment. With increasing clock rates and increasingly fast computers, the transmission of electromagnetic waves through such arrays is becoming an increasingly severe problem. Whereas the isolated aperture has been the subject of extensive research [2–22], the modeling of multiple interacting apertures has been little addressed [23–26]. Through the application of Babinet's principle the scattering from an array of circular disks, which finds application in the theory of artificial dielectrics, is a related problem. In [23] the interaction in an infinite periodic array

of circular disks is solved assuming dipole fields. In [24] transmission through an infinite periodic lattice of rectangular apertures is solved through a variational approach. In [25] transmission through an infinite periodic lattice of apertures in an infinitely thin screen is solved via the moment method, and in [26] the same problem is solved for apertures in a thick screen. All of the above referenced work is concerned with infinite arrays. We consider here an arbitrary finite array of circular apertures in a thin screen, and this problem implemented in the FDTD technique, where it is then easily coupled to more complex configurations. The purpose of this paper is to extend the isolated aperture formulation to model arrays of closely-spaced apertures. As in the isolated aperture formulation [1], the present formulation assumes apertures in an infinite perfectly-conducting thin screen, but is applicable to apertures in a finite screen.

We begin in Section 2 with a look at an analytical solution based on interacting electric and magnetic dipoles, which applies to an arbitrary array of apertures, and this solution is compared with the solution for an infinite array of apertures. In Section 3 we modify the isolated aperture formulation to allow sources on both sides of the screen, since for multiple apertures the fields transmitted by one aperture can excite another aperture from the back, or transmission, side of the screen. The formulation for sources on both sides of the screen follows directly from the superposition principle. The isolated aperture formulation, modified so as to allow sources on both sides of the screen, can be applied with high accuracy to an array of apertures, provided the apertures are spaced at least two grid cells apart. For closely spaced apertures, that is, apertures spaced one grid cell apart, the isolated aperture method can lead to an error in transmitted power in excess of ten percent. This error is due to inaccuracies in the FDTD dipole fields. In Section 4 we present a method to subtract the effect of error in the FDTD dipole fields. The correction is based on an analytical solution of the FDTD equations for dipole radiation. In Section 5 we evaluate the method, comparing the FDTD solution with the analytical solution.

2. Analytical Solution for a Finite Array of Apertures

An example geometry of multiple interacting apertures is illustrated in Figure 1, which indicates a plane wave incident on an aperture perforated screen. Alternately, as shown in the figure, we may have a

dipole of moment Il radiating in the presence of the screen. To test the accuracy of the multiple aperture method presented here we employ an analytical solution. An analytical solution is here presented which is applicable to an array of interacting, perhaps closely spaced, apertures. The solution is obtained by approximating the aperture array fields to be that of an array of electric and magnetic dipoles which represent the apertures according to Bethe's hole theory [19]. This approximation is here referred to as the dipole approximation. For large closely-spaced apertures higher order multipole interaction becomes important, and hence the importance of the multipole terms is assessed so as to determine the range of validity of the dipole approximation.

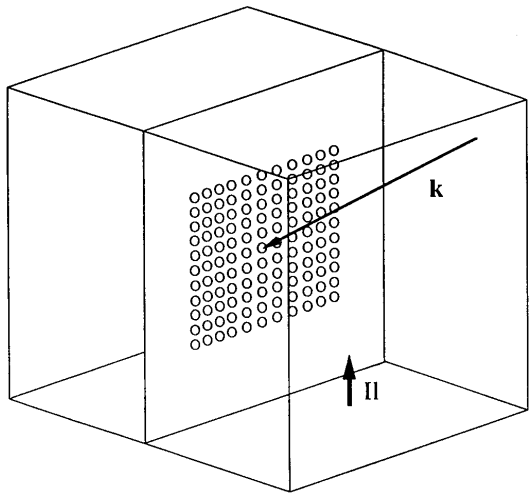

Figure 1. Geometry of multiple interacting apertures.

The simplest treatment of an array of apertures is to consider them as being independent, or non-interacting. For this case the surface magnetic currents representing the aperture fields are the same as the fields of an isolated aperture, and to high accuracy the aperture fields are given by the Rayleigh series solution [2,22]. The effect of aperture interaction is here assessed by comparing the magnetic surface currents and transmitted power with those values for the independent, or non-interacting, apertures.

The Rayleigh series solution for the circular aperture fields is determined by the total short-circuit electric and magnetic fields at the

center of the aperture. The short-circuit field at the center of each aperture is the short-circuit field due to the incident wave plus the short circuit fields produced by all the other apertures, including the coupling from the back side of the screen. The geometry of this problem is shown in Figure 2.

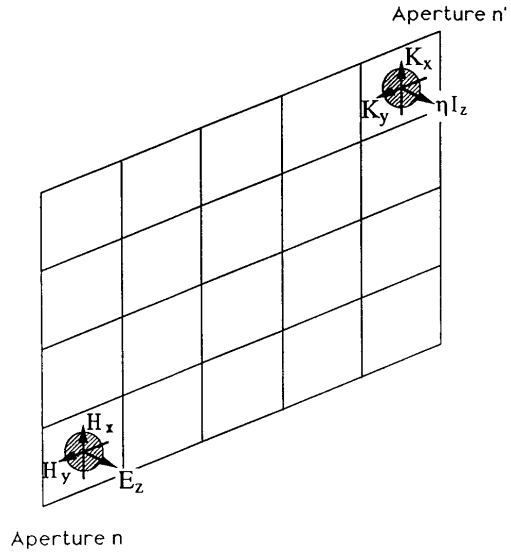

Figure 2. Dipole approximation geometry.

Denoting the magnetic surface current K_x at the nth aperture as $(K_x)_n$, and the electric field e_z^{sc} at the center of the nth aperture as $(e_z^{sc})_n$, etc., we can write,

$$(K_x)_n = -ik\Delta^2\gamma_m\epsilon(h_x^{sc})_n + \gamma_m\epsilon\sum_{n'\neq n}\left[L_{nn'}^{xx}(K_x)_{n'} + L_{nn'}^{xy}(K_y)_{n'} + L_{nn'}^{xz}(\eta I_z)_{n'}\right] \quad (1)$$

$$(K_y)_n = -ik\Delta^2\gamma_m\epsilon(h_y^{sc})_n + \gamma_m\epsilon\sum_{n'\neq n}\left[L_{nn'}^{yx}(K_x)_{n'} + L_{nn'}^{yy}(K_y)_{n'} + L_{nn'}^{yz}(\eta I_z)_{n'}\right] \quad (2)$$

$$(\eta I_z)_n = +ik\Delta^2\gamma_e\epsilon(e_z^{sc})_n - \gamma_e\epsilon\sum_{n'\neq n}\left[L_{nn'}^{zx}(K_x)_{n'} + L_{nn'}^{zy}(K_y)_{n'} + L_{nn'}^{zz}(\eta I_z)_{n'}\right] \quad (3)$$

where $\alpha_e = \gamma_e a^3$ and $\alpha_m = \gamma_m a^3$ are the electric and magnetic polarizabilities [7] of the aperture; $\epsilon \equiv (\frac{a}{\Delta})^3$ is regarded as a small parameter; a is the radius of the aperture and Δ the grid spacing; $e_z^{sc} = E_z^{sc}$ and $h_i^{sc} = \eta H_i^{sc}$ are the normalized electric and magnetic fields; and I_z and K_i are the electric and magnetic currents representing the aperture. For a small circular aperture $\gamma_e = 2/3$ and $\gamma_m = 4/3$. In the above,

$$L_{nn'}^{xx} = \frac{1}{\pi}\left(\frac{\Delta}{r}\right)^3 \left\{ -1 + ikr - (ikr)^2 + \left(\frac{x}{r}\right)^2 [3 - 3ikr + (ikr)^2] \right\} e^{ikr} \quad (4)$$

$$L_{nn'}^{xy} = \frac{1}{\pi}\left(\frac{\Delta}{r}\right)^3 \left(\frac{xy}{r^2}\right) [3 - 3ikr + (ikr)^2] e^{ikr} \quad (5)$$

$$L_{nn'}^{xz} = \frac{iky}{\pi}\left(\frac{\Delta}{r}\right)^3 (1 - ikr) e^{ikr} \quad (6)$$

$$L_{nn'}^{yx} = \frac{1}{\pi}\left(\frac{\Delta}{r}\right)^3 \left(\frac{xy}{r^2}\right) [3 - 3ikr + (ikr)^2] e^{ikr} \quad (7)$$

$$L_{nn'}^{yy} = \frac{1}{\pi}\left(\frac{\Delta}{r}\right)^3 \left\{ -1 + ikr - (ikr)^2 + \left(\frac{y}{r}\right)^2 [3 - 3ikr + (ikr)^2] \right\} e^{ikr} \quad (8)$$

$$L_{nn'}^{yz} = \frac{-ikx}{\pi}\left(\frac{\Delta}{r}\right)^3 (1 - ikr) e^{ikr} \quad (9)$$

$$L_{nn'}^{zx} = \frac{iky}{\pi}\left(\frac{\Delta}{r}\right)^3 (1 - ikr) e^{ikr} \quad (10)$$

$$L_{nn'}^{zy} = \frac{-ikx}{\pi}\left(\frac{\Delta}{r}\right)^3 (1 - ikr) e^{ikr} \quad (11)$$

$$L_{nn'}^{zz} = \frac{1}{\pi}\left(\frac{\Delta}{r}\right)^3 \left\{ -1 + ikr - (ikr)^2 \right\} e^{ikr} \quad (12)$$

give the dipole fields of the n'th aperture at the center of aperture n, including the contribution from the transmitted fields of the other apertures. Also, $r \equiv r_{nn'}$ is the distance between the centers of apertures n and n', and x and y are the distances in the x and y directions between the two apertures. In order to write (1)–(3) as a

matrix multiplication, we define,

$$M_{nn'}^{ab} = \begin{cases} L_{nn'}^{ab} & \text{if } n \neq n' \\ 0 & \text{otherwise} \end{cases} \tag{13}$$

The above equations can now be represented by a matrix equation with the following definitions,

$$\overline{\overline{M}}^{ab} = \begin{bmatrix} M_{11}^{ab} & M_{12}^{ab} & \dots & M_{1N}^{ab} \\ M_{21}^{ab} & M_{22}^{ab} & \dots & M_{2N}^{ab} \\ \vdots & \vdots & \ddots & \vdots \\ M_{N1}^{ab} & M_{N2}^{ab} & \dots & M_{NN}^{ab} \end{bmatrix} \tag{14}$$

$$a, b = x, y, z \tag{15}$$

$$\overline{F}_x^{sc} = \begin{bmatrix} -ik\Delta^2(h_x^{sc})_1 \\ -ik\Delta^2(h_x^{sc})_2 \\ \vdots \\ -ik\Delta^2(h_x^{sc})_N \end{bmatrix} \tag{16}$$

$$\overline{F}_y^{sc} = \begin{bmatrix} -ik\Delta^2(h_y^{sc})_1 \\ -ik\Delta^2(h_y^{sc})_2 \\ \vdots \\ -ik\Delta^2(h_y^{sc})_N \end{bmatrix} \tag{17}$$

$$\overline{F}_z^{sc} = \begin{bmatrix} -ik\Delta^2(e_z^{sc})_1 \\ -ik\Delta^2(e_z^{sc})_2 \\ \vdots \\ -ik\Delta^2(e_z^{sc})_N \end{bmatrix} \tag{18}$$

$$\overline{K}_x = \begin{bmatrix} (K_x)_1 \\ (K_x)_2 \\ \vdots \\ (K_x)_N \end{bmatrix} \tag{19}$$

$$\overline{K}_y = \begin{bmatrix} (K_y)_1 \\ (K_y)_2 \\ \vdots \\ (K_y)_N \end{bmatrix} \tag{20}$$

$$\eta\overline{I}_z = \begin{bmatrix} \eta(I_z)_1 \\ \eta(I_z)_2 \\ \vdots \\ \eta(I_z)_N \end{bmatrix} \tag{21}$$

With these definitions Equations (1)–(3) can be written in block matrix form as,

$$\begin{bmatrix} \overline{K}_x \\ \overline{K}_y \\ \eta\overline{I}_z \end{bmatrix} = \epsilon\overline{\overline{\gamma}} \cdot \begin{bmatrix} \overline{F}_x^{sc} \\ \overline{F}_y^{sc} \\ \overline{F}_z^{sc} \end{bmatrix} + \epsilon\overline{\overline{\gamma}} \cdot \begin{bmatrix} \overline{\overline{M}}^{xx} & \overline{\overline{M}}^{xy} & \overline{\overline{M}}^{xz} \\ \overline{\overline{M}}^{yx} & \overline{\overline{M}}^{yy} & \overline{\overline{M}}^{yz} \\ \overline{\overline{M}}^{zx} & \overline{\overline{M}}^{zy} & \overline{\overline{M}}^{zz} \end{bmatrix} \cdot \begin{bmatrix} \overline{K}_x \\ \overline{K}_y \\ \eta\overline{I}_z \end{bmatrix} \tag{22}$$

where,

$$\overline{\overline{\gamma}} = \begin{bmatrix} \gamma_m\overline{\overline{I}} & 0 & 0 \\ 0 & \gamma_m\overline{\overline{I}} & 0 \\ 0 & 0 & -\gamma_e\overline{\overline{I}} \end{bmatrix} \tag{23}$$

The aperture currents are then given by,

$$\overline{K} = \epsilon\overline{\overline{\gamma}} \cdot \overline{F}^{sc} + \epsilon\overline{\overline{\gamma}} \cdot \overline{\overline{M}} \cdot \overline{K} \tag{24}$$

$$= (\overline{\overline{I}} - \epsilon\overline{\overline{\gamma}} \cdot \overline{\overline{M}})^{-1} \cdot \epsilon\overline{\overline{\gamma}} \cdot \overline{F}^{sc} \tag{25}$$

$$= (\overline{\overline{I}} + \epsilon\overline{\overline{\gamma}} \cdot \overline{\overline{M}} + \epsilon^2(\overline{\overline{\gamma}} \cdot \overline{\overline{M}})^2 + \cdots) \cdot \epsilon\overline{\overline{\gamma}} \cdot \overline{F}^{sc} \tag{26}$$

where,

$$\overline{F}^{sc} = \begin{bmatrix} \overline{F}_x^{sc} \\ \overline{F}_y^{sc} \\ \overline{F}_z^{sc} \end{bmatrix} \tag{27}$$

$$\overline{K} = \begin{bmatrix} \overline{K}_x \\ \overline{K}_y \\ \eta \overline{I}_z \end{bmatrix} \tag{28}$$

$$\overline{\overline{M}} = \begin{bmatrix} \overline{\overline{M}}^{xx} & \overline{\overline{M}}^{xy} & \overline{\overline{M}}^{xz} \\ \overline{\overline{M}}^{yx} & \overline{\overline{M}}^{yy} & \overline{\overline{M}}^{yz} \\ \overline{\overline{M}}^{zx} & \overline{\overline{M}}^{zy} & \overline{\overline{M}}^{zz} \end{bmatrix} \tag{29}$$

The power transmitted by the aperture array is equal to the power radiated by the equivalent dipoles in the presence of the perfect conductor. From the complex Poynting vector theorem the transmitted power is given by,

$$P = \frac{(k\Delta)^2}{6\pi\eta} \overline{K}^{\dagger} \cdot \overline{K} + \frac{1}{2\eta(k\Delta)} \mathrm{Im}\{\overline{K}^{\dagger} \cdot \overline{\overline{M}} \cdot \overline{K}\} \tag{30}$$

The effect of aperture interaction is illustrated in Tables 1–4 for a 5×5 array of closely spaced apertures. The tables give the percentage increase in the aperture magnetic current over the isolated aperture value for two aperture sizes, a/Δ, and two frequencies, $\Delta/\lambda = .05$ and $\Delta/\lambda = .1$, which correspond respectively to twenty and ten grid cells per wavelength. The tables indicate that the magnetic currents increase with both frequency and aperture radius, and the increase with radius is proportional to $(a/\Delta)^3$. The effect of interaction is to increase the magnetic currents by as much as 24%.

K_x	1	2	3	4	5
1	1.39	2.82	3.01	2.82	1.39
2	1.10	2.66	2.91	2.66	1.10
3	1.10	2.64	2.90	2.64	1.10
4	1.10	2.66	2.91	2.66	1.10
5	1.39	2.82	3.01	2.82	1.39

Table 1. Percentage increase in the aperture magnetic current over the isolated aperture value for $\Delta/\lambda = .05$, $a/\Delta = .25$.

K_x	1	2	3	4	5
1	1.25	2.95	3.22	2.95	1.25
2	1.30	3.24	3.61	3.24	1.30
3	1.40	3.36	3.75	3.36	1.40
4	1.30	3.24	3.61	3.24	1.30
5	1.25	2.95	3.22	2.95	1.25

Table 2. Percentage increase in the aperture magnetic current over the isolated aperture value for $\Delta/\lambda = .1$, $a/\Delta = .25$.

K_x	1	2	3	4	5
1	9.65	18.34	19.86	18.34	9.65
2	7.75	17.04	18.89	17.04	7.75
3	7.77	16.94	18.82	16.94	7.77
4	7.75	17.04	18.89	17.04	7.75
5	9.65	18.34	19.86	18.34	9.65

Table 3. Percentage increase in the aperture magnetic current over the isolated aperture value for $\Delta/\lambda = .05$, $a/\Delta = .45$.

K_x	1	2	3	4	5
1	8.52	18.74	20.82	18.74	8.52
2	8.92	20.65	23.38	20.65	8.92
3	9.65	21.54	24.39	21.54	9.65
4	8.92	20.65	23.38	20.65	8.92
5	8.52	18.74	20.82	18.74	8.52

Table 4. Percentage increase in the aperture magnetic current over the isolated aperture value for $\Delta/\lambda = .1$, $a/\Delta = .45$.

Through Babinet's principle we can compare the finite array results with those given in [23] for an infinite array of disks. The electric polarizability of the disk is [21] $\alpha_e = 16a^3/3$. Applying Babinet's principle to the array of disks we find that the induced magnetic currents for an infinite array of circular apertures are given by,

$$K_i l = \frac{\alpha_e/4}{1 - \alpha_e C_{ee}} \frac{\partial h_i^{sc}}{\partial \tau} \tag{31}$$

where α_e is the *disk* polarizability, which is different than the aperture polarizability. For normal incidence the interaction constant C_{ee} is given as [23],

$$\begin{aligned} C_{ee} = \frac{1}{\pi\Delta^3} \Bigg\{ & 1.2 - 2\sum_{m=1}^{\infty}\sum_{n=1}^{\infty} (\gamma_n\Delta)^2 K_0(m\gamma_n\Delta) \\ & + (k\Delta)^2 \Bigg[-0.727 + \frac{1}{2}\sum_{m=1}^{\infty}\left(\frac{2\pi}{\gamma_m\Delta} - \frac{1}{m}\right)\Bigg] \\ & + \frac{1}{96}(k\Delta)^4 + i\left[\frac{\pi}{2}(k\Delta) - \frac{1}{6}(k\Delta)^3\right]\Bigg\} \end{aligned} \tag{32}$$

where $\gamma_n^2 = (2n\pi)^2 - k^2$ and K_0 is the modified Bessel function. The increase in the magnetic currents due to interaction is given by $(1 - \alpha_e C_{ee})^{-1}$, which is presented in Table 5 below.

a/Δ	$\Delta/\lambda = 0$	$\Delta/\lambda = 0.05$	$\Delta/\lambda = 0.1$
0.25	3.3	2.9	2.3
0.45	22.8	19.0	13.4

Table 5. Percentage increase in the aperture magnetic current over the isolated aperture value for an infinite array of apertures.

These results compare well with the results in Tables 1–4 when $\Delta/\lambda = 0.05$. For higher frequencies ($\Delta/\lambda = 0.1$) the finite aperture array results are strongly dependent on the size of the aperture array. For large arrays the finite array results approach those for the infinite array.

A rough idea of the attenuation which can be expected from an array of apertures can be inferred form the transmission coefficient for an infinite array of apertures, which appears to a plane wave as a shunt susceptance [27]. The transmission coefficient for an infinite array of interacting apertures can be shown to be,

$$T = -ik\Delta \frac{\frac{8}{3}(a/\Delta)^3}{1 - \frac{16}{3}(a/\Delta)^3 C_{ee}\Delta^3} \tag{33}$$

Before proceeding to the FDTD implementation of multiple interacting apertures we consider the effect of the higher-order multipole interaction between the apertures. Our objective here is to assess the error in neglecting these higher-order interactions.

From the preceding analysis we know that the currents at the n th aperture, within the Rayleigh series approximation to order ka, are induced by the fields at the center of the aperture, and these fields include the short-circuit field due to the incident and reflected waves, and, in addition, the fields scattered from the other apertures. In the above analysis the fields scattered from the other apertures are approximated as dipole fields. For closely-spaced apertures, however, the higher-order multipole fields from neighboring apertures become important. These higher-order fields decay rapidly away from the center of the aperture, and hence we suspect the higher-order interaction to be important only for large, closely-spaced, apertures. In the following we restrict ourselves to the case of normal incidence, where only a magnetic dipole moment is induced, and consider the strength of the magnetic fields from the nearest-neighbor apertures for apertures spaced

one per FDTD cell. To assess the error in neglecting higher-order interactions, we determine the magnetic field due to the higher-order multipoles and compare this field with the total magnetic field comprised of the short-circuit field, dipole fields, and higher-order multipole fields. The higher-order terms considered are the magnetic quadrupole, electric quadrupole and magnetic octupole terms.

To lowest order in frequency, the magnetic field close to a circular aperture is given by,

$$ikh_x = \frac{1}{\pi}\iint_{S'} dS' \left\{ \frac{(y-y')^2 - 2(x-x')^2}{R^5} M_{sx}(\overline{\rho}') - \frac{3(x-x')(y-y')}{R^5} M_{sy}(\overline{\rho}') \right\} \tag{34}$$

where $R \equiv \sqrt{(x-x')^2 + (y-y')^2}$. In the above the field from the magnetic current on the back side of the screen has been included. This integral is of the form,

$$\iint_A dS\overline{F} \cdot \overline{M} = \iint_A dS F_\alpha M_\alpha \tag{35}$$

where the summation convention is implied on the repeated indices. Expanding $\overline{F}$ in a Taylor series expansion gives,

$$\begin{aligned} \iint_A dS\overline{F} \cdot \overline{M} = F_\alpha(0) \iint_A dS M_\alpha + \frac{\partial F_\alpha}{\partial x_\beta}(0) \iint_A dS x_\beta M_\alpha \\ + \tfrac{1}{2} \frac{\partial^2 F_\alpha}{\partial x_\beta \partial x_\gamma}(0) \iint_A dS x_\beta x_\gamma M_\alpha \end{aligned} \tag{36}$$

The first term is the magnetic dipole contribution; the second term contains the electric dipole and magnetic quadrupole contributions; and the third term contains the electric quadrupole and magnetic octupole contributions. These integrals can be evaluated from the equivalent magnetic surface currents given in [1]. After a little algebra the magnetic field can be written as,

$$h_x = h_x^{sc} + \frac{8}{3\pi}\left\{ (1 + \frac{1}{2\sqrt{2}})(\frac{a}{\Delta})^3 - 13(1 - \frac{11}{26\sqrt{2}})(\frac{a}{\Delta})^5 \right\} h_x^{sc} \tag{37}$$

where the second term above is the magnetic dipole contribution, and the third term represents the electric quadrupole and magnetic octupole contributions. The electric dipole and magnetic quadrupole contributions are zero. The above expression results from evaluating the

various partial derivatives of $\overline{F}$ at the center of the aperture, and summing contributions from the eight nearest neighbors. From the above we find that the ratio of the higher-order contributions to the dipole contribution is given by $6.73(a/\Delta)^2$, which is quite large, giving for $a/\Delta = .45$ a ratio of 1.36. Hence, for large apertures the higher-order contributions are larger than the dipole contribution. The total error in neglecting the higher-order contributions is approximately $7.73(a/\Delta)^5$, which for $a/\Delta = .45$ gives an error of $.143$. For this case the total transmitted power is in error by about $28\,\%$. The higher-order multipole interaction consequently places a restriction on how large the aperture radius can be for closely-spaced apertures. For the error in total transmitted power to be less than 10%, for example, we must have $a/\Delta < .37$. In closing, we observe that it is possible, through a more detailed analysis of the higher-order interaction, to correct for the above error.

3. Isolated Aperture Formulation for Sources on Both Sides of the Screen

When sources are present on both sides of the screen the induced currents from the superposition principle are given by,

$$K_x^{(-)} = \frac{\alpha_m}{\Delta}\eta\left(\frac{\partial H_x^{sc\,(-)}}{\partial\tau} - \frac{\partial H_x^{sc\,(+)}}{\partial\tau}\right) \tag{38}$$

$$K_y^{(-)} = \frac{\alpha_m}{\Delta}\eta\left(\frac{\partial H_y^{sc\,(-)}}{\partial\tau} - \frac{\partial H_y^{sc\,(+)}}{\partial\tau}\right) \tag{39}$$

$$\eta I_z^{(-)} = -\frac{\alpha_e}{\Delta}\left(\frac{\partial E_z^{sc\,(-)}}{\partial\tau} - \frac{\partial E_z^{sc\,(+)}}{\partial\tau}\right) \tag{40}$$

where the $(\pm)$ superscript indicates the short-circuit fields on the $\pm z$ side of the screen. Alternately, the induced currents on the $+z$ side of the screen are given by,

$$K_x^{(+)} = \frac{\alpha_m}{\Delta}\eta\left(\frac{\partial H_x^{sc\,(+)}}{\partial\tau} - \frac{\partial H_x^{sc\,(-)}}{\partial\tau}\right) \tag{41}$$

$$K_y^{(+)} = \frac{\alpha_m}{\Delta}\eta\left(\frac{\partial H_y^{sc\,(+)}}{\partial\tau} - \frac{\partial H_y^{sc\,(-)}}{\partial\tau}\right) \tag{42}$$

$$\eta I_z^{(+)} = -\frac{\alpha_e}{\Delta}\left(\frac{\partial E_z^{sc\,(+)}}{\partial\tau} - \frac{\partial E_z^{sc\,(-)}}{\partial\tau}\right) \tag{43}$$

The FDTD implementation of the above equations for a thin screen at $z = 0$ is,

$$\begin{aligned}\tilde{K}_x^p(l,m,0) \equiv \frac{\alpha_m}{\Delta^2}[&\frac{4}{3}e_y^p(l,m,1) - \frac{1}{6}e_y^p(l,m,2) - e_z^p(l,m+1,0)\\ &+ e_z^p(l,m,0) + \frac{4}{3}e_y^p(l,m,-1) - \frac{1}{6}e_y^p(l,m,-2)\\ &+ e_z^p(l,m+1,-1) - e_z^p(l,m,-1)] \qquad (44)\\ \tilde{K}_y^p(l,m,0) \equiv \frac{\alpha_m}{\Delta^2}[&-\frac{4}{3}e_x^p(l,m,1) + \frac{1}{6}e_x^p(l,m,2) + e_z^p(l+1,m,0)\\ &- e_z^p(l,m,0) - \frac{4}{3}e_x^p(l,m,-1) + \frac{1}{6}e_x^p(l,m,-2)\\ &- e_z^p(l+1,m,-1) + e_z^p(l,m,-1)] \qquad (45)\\ \eta\tilde{I}_z^p(l,m,0) = &-\frac{\alpha_e}{\Delta^2}[h_y^{p-1}(l,m,0) - h_y^{p-1}(l-1,m,0)\\ &+ h_x^{p-1}(l,m-1,0) - h_x^{p-1}(l,m,0)\\ &- h_y^{p-1}(l,m,-1) + h_y^{p-1}(l-1,m,-1)\\ &- h_x^{p-1}(l,m-1,-1) + h_x^{p-1}(l,m,-1)] \qquad (46)\end{aligned}$$

where the tilde indicates the currents induced by the incident and reflected fields alone. Using these equations without a correction to subtract the dipole fields gives twice the error as the previous formulation [1], which allowed sources on one side of the screen only. The additional error results from the dipole fields on the opposite side of the screen. In the previous formulation the dipole fields were present but did not induce currents, being on the transmission side of the screen. In the present formulation, however, the dipole fields on the transmission side of the screen do induce currents, and the currents induced are equal to the currents induced from the dipole fields on the incident side of the screen. Hence, in the present formulation both dipole fields must be subtracted.

The induced dipole currents with corrections for the dipole fields on both sides of the screen are,

$$K_x = \frac{\alpha_m}{\Delta}\left[\left(\frac{\partial h_x^{(+)}}{\partial\tau} - \frac{\partial h_x^{(-)}}{\partial\tau}\right) - \left(\frac{\partial h_{dx}^{(+)}}{\partial\tau} - \frac{\partial h_{dx}^{(-)}}{\partial\tau}\right)\right] \qquad (47)$$

$$K_y = \frac{\alpha_m}{\Delta}\left[\left(\frac{\partial h_y^{(+)}}{\partial\tau} - \frac{\partial h_y^{(-)}}{\partial\tau}\right) - \left(\frac{\partial h_{dy}^{(+)}}{\partial\tau} - \frac{\partial h_{dy}^{(-)}}{\partial\tau}\right)\right] \qquad (48)$$

$$\eta I_z = -\frac{\alpha_e}{\Delta}\left[\left(\frac{\partial e_z^{(+)}}{\partial \tau} - \frac{\partial e_z^{(-)}}{\partial \tau}\right) - \left(\frac{\partial e_{dz}^{(+)}}{\partial \tau} - \frac{\partial e_{dz}^{(-)}}{\partial \tau}\right)\right] \tag{49}$$

where the $(+)$ superscripts on the currents have been dropped. The induced currents on the $-z$ side of the screen are the negative of the above. Since the dipoles on the transmission side of the screen are opposite the dipoles on the incident side, we have,

$$h_{dx}^{(-)} = -\, h_{dx}^{(+)} \tag{50}$$

$$h_{dy}^{(-)} = -\, h_{dy}^{(+)} \tag{51}$$

$$e_{dz}^{(-)} = -\, e_{dz}^{(+)} \tag{52}$$

and, hence, it is evident that the corrected equations will be identical with those given in [1] except that now the correction coefficients are twice the previous values. The corrected equations, then, including sources on both sides of the screen are,

$$\begin{aligned} K_x^p = &+ \alpha_2\left(\frac{a}{\Delta}\right)^3(\eta\tilde{I}_z^p - \eta\tilde{I}_z^{p-1}) + [1 - \alpha_4\left(\frac{a}{\Delta}\right)^3]\tilde{K}_x^p \\ &+ \alpha_5\left(\frac{a}{\Delta}\right)^3\tilde{K}_y^p \end{aligned} \tag{53}$$

$$\begin{aligned} K_y^p = &- \alpha_2\left(\frac{a}{\Delta}\right)^3(\eta\tilde{I}_z^p - \eta\tilde{I}_z^{p-1}) + \alpha_5\left(\frac{a}{\Delta}\right)^3\tilde{K}_x^p \\ &+ [1 - \alpha_4\left(\frac{a}{\Delta}\right)^3]\tilde{K}_y^p \end{aligned} \tag{54}$$

$$\eta I_z^p = [1 + \alpha_1\left(\frac{a}{\Delta}\right)^3]\eta\tilde{I}_z^p + \alpha_3\left(\frac{a}{\Delta}\right)^3(\tilde{K}_x^p - \tilde{K}_x^{p-1}) \tag{55}$$

where $\tilde{K}_x^p = \tilde{K}_x^p(l,m,n)$, $\tilde{K}_y^p = \tilde{K}_y^p(l,m,n)$ and $\tilde{I}_z^p = \tilde{I}_z^p(l,m,n)$ are given above, and,

$$\alpha_1 \equiv \frac{8\gamma_e(2\sigma_1)}{\pi^2} \tag{56}$$

$$\alpha_2 \equiv \frac{2\gamma_m(2\sigma_1)}{\pi^2}\left(\frac{\Delta}{\Delta\tau}\right) \tag{57}$$

$$\alpha_3 \equiv \frac{4\gamma_e(2\sigma_2)}{\pi^2}\left(\frac{\Delta}{\Delta\tau}\right) \tag{58}$$

$$\alpha_4 \equiv \frac{8\gamma_m(2\sigma_3)}{\pi^2} \tag{59}$$

$$\alpha_5 \equiv \frac{8\gamma_m(2\sigma_4)}{\pi^2} \tag{60}$$

4. Correcting the FDTD Dipole Fields

The FDTD algorithm automatically accounts for all aperture interactions, and from this observation we expect the isolated aperture approach to apply for aperture arrays since it correctly subtracts the self-field of the aperture while retaining the contributions from all other apertures. While this is true for apertures spaced at least two cells apart, it turns out, however, that a sizable error results for closely spaced apertures. The reason for the error is that the FDTD aperture-scattered fields are not accurate near the aperture, and hence there is an error in the interaction fields for closely spaced apertures. The sources of the error in the FDTD aperture-scattered fields near the aperture are many. To begin with, an aperture is correctly modeled by equivalent electric and magnetic dipoles only for distances sufficiently far from the aperture. We do not attempt here, however, to correct for this error. As noted above, this places a restriction on how large the aperture radius can be. The results that are presented below are compared to the dipole approximation to multiple interacting apertures, and hence our goal here to accurately render this approximation in the FDTD algorithm. The remaining sources of the error are in the dipole fields. Figure 2 illustrates the fields H_x, H_y and E_z produced by currents K_x, K_y and ηI_z in the analytical solution. In the discretized space of the FDTD technique, however, the geometry is as shown in Figure 3. From these two figures it is evident that the FDTD dipole fields will differ from the analytical dipole fields. The reasons for the discrepancies are: (1) the dipoles K_x, K_y and ηI_z and their image dipoles are not coincident as in the analytical solution, but are separated a distance Δ; (2) the FDTD fields close to a dipole deviate from the continuum values; and (3) the dipoles K_x, K_y and ηI_z are displaced from the center of the aperture. All of these sources of error are significant only for closely spaced apertures.

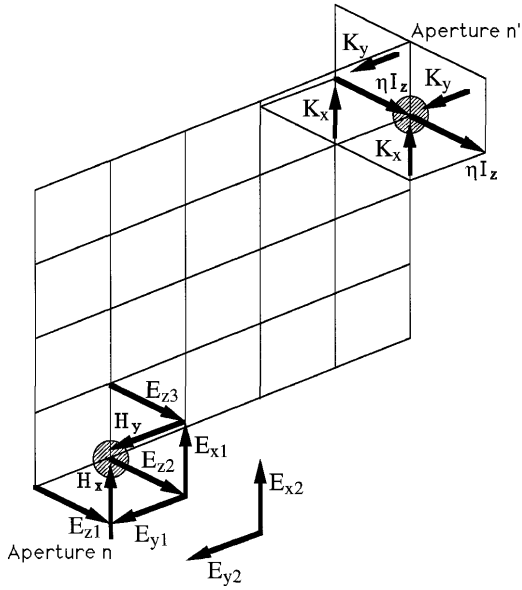

Figure 3. FDTD dipole geometry.

Our approach to correcting the dipole fields is to analytically subtract out the FDTD fields which are incorrect and to add back the correct fields. For simplicity we consider here a rectangular array of apertures, although the method can be applied to an arbitrary array of apertures. The fields at aperture n are due to the short-circuit field and the fields from all other apertures $n' \neq n$, and, as in the isolated apertures case, the fields from aperture n itself as well. Since the aperture interaction fields are incorrect only for close apertures, the above correction is applied only for the eight nearest neighbors, n', of aperture n, and it is assumed that the induced currents at aperture n' are the same as those at aperture n. In addition, since the correction is applied to close apertures only, we need to keep terms only to lowest order in frequency.

For simplicity the above correction is applied to all apertures, including those along the edges and at the corners of the aperture array, even though for these apertures, which do not have eight immediate neighbors, the correction does not apply. Different corrections can be derived for edge and corner apertures, but it is evident from the results given below that the error due to neglecting the different environments of the edge and corner apertures is small.

Proceeding, then, with the above approach, to lowest order in frequency we have,

$$L^{xx}_{nn'} = \frac{1}{\pi}\left(\frac{\Delta}{r}\right)^3\left\{-1+3\left(\frac{x}{r}\right)^2\right\} \tag{61}$$

$$L^{xy}_{nn'} = \frac{1}{\pi}\left(\frac{\Delta}{r}\right)^3\left(\frac{3xy}{r^2}\right) \tag{62}$$

$$L^{xz}_{nn'} = \frac{iky}{\pi}\left(\frac{\Delta}{r}\right)^3 \tag{63}$$

$$L^{yx}_{nn'} = L^{xy}_{nn'} \tag{64}$$

$$L^{yy}_{nn'} = \frac{1}{\pi}\left(\frac{\Delta}{r}\right)^3\left\{-1+3\left(\frac{y}{r}\right)^2\right\} \tag{65}$$

$$L^{yz}_{nn'} = \frac{-ikx}{\pi}\left(\frac{\Delta}{r}\right)^3 \tag{66}$$

$$L^{zx}_{nn'} = L^{xz}_{nn'} \tag{67}$$

$$L^{zy}_{nn'} = L^{yz}_{nn'} \tag{68}$$

$$L^{zz}_{nn'} = -\frac{1}{\pi}\left(\frac{\Delta}{r}\right)^3 \tag{69}$$

The analytical dipole fields from the eight nearest neighbors n' to n are,

$$\left(\frac{\partial h_{dx}}{\partial \tau}\right)^{ANAL} = \left(\sum_{n'\neq n} L^{xx}_{nn'}\right)K_x + \left(\sum_{n'\neq n} L^{xy}_{nn'}\right)K_y + \left(\sum_{n'\neq n} L^{xz}_{nn'}\right)\eta I_z \tag{70}$$

$$\left(\frac{\partial h_{dy}}{\partial \tau}\right)^{ANAL} = \left(\sum_{n'\neq n} L^{yx}_{nn'}\right)K_x + \left(\sum_{n'\neq n} L^{yy}_{nn'}\right)K_y + \left(\sum_{n'\neq n} L^{yz}_{nn'}\right)\eta I_z \tag{71}$$

$$\left(\frac{\partial e_{dz}}{\partial \tau}\right)^{ANAL} = \left(\sum_{n' \neq n} L^{zx}_{nn'}\right) K_x + \left(\sum_{n' \neq n} L^{zy}_{nn'}\right) K_y + \left(\sum_{n' \neq n} L^{zz}_{nn'}\right) \eta I_z \tag{72}$$

which from Equations (61)–(69) can be evaluated as,

$$\Delta^2 \left(\frac{\partial h_{dx}}{\partial \tau}\right)^{ANAL} = \frac{8\sigma_0}{\pi^2} K_x \tag{73}$$

$$\Delta^2 \left(\frac{\partial h_{dy}}{\partial \tau}\right)^{ANAL} = \frac{8\sigma_0}{\pi^2} K_y \tag{74}$$

$$\Delta^2 \left(\frac{\partial e_{dz}}{\partial \tau}\right)^{ANAL} = \frac{-16\sigma_0}{\pi^2} \eta I_z \tag{75}$$

$$\sigma_0 \equiv \frac{\pi}{2}\left[1 + \frac{1}{2\sqrt{2}}\right] = 2.12616 \tag{76}$$

In an analysis identical to that for the isolated aperture [1], the FDTD dipole fields for an array of $(2N+1) \times (2N+1)$ apertures, N an integer, are given analytically as,

$$\Delta^2 \left(\frac{\partial h_{dx}}{\partial \tau}\right)^{FDTD} + 2K_x = \frac{8}{\pi^2}(\sigma_3 K_x - \sigma_4 K_y) - \frac{2\sigma_1}{\pi^2}(-ik\Delta)\eta I_z \tag{77}$$

$$\Delta^2 \left(\frac{\partial h_{dy}}{\partial \tau}\right)^{FDTD} + 2K_y = \frac{8}{\pi^2}(-\sigma_4 K_x + \sigma_3 K_y) + \frac{2\sigma_1}{\pi^2}(-ik\Delta)\eta I_z \tag{78}$$

$$\Delta^2 \left(\frac{\partial e_{dz}}{\partial \tau}\right)^{FDTD} + 2\eta I_z = \frac{4\sigma_2}{\pi^2}(-ik\Delta)(K_x - K_y) + \frac{8\sigma_1}{\pi^2}\eta I_z \tag{79}$$

The constants σ_n, however, are different than the corresponding constants for an isolated aperture given in [1], representing now the fields of the aperture array, and are given by,

$$\sigma_1 \equiv 2\int_0^{\frac{\pi}{2}} dx \int_0^{\frac{\pi}{2}} dy F \cdot \frac{\sin[(2N+1)x]}{\sin x} \cdot \frac{\sin[(2N+1)y]}{\sin y} \cdot [G-F] \quad (80)$$

$$= 1.22651 \quad (81)$$

$$\sigma_2 \equiv 2\int_0^{\frac{\pi}{2}} dx \int_0^{\frac{\pi}{2}} dy \frac{\sin^2 y \cos^2 x}{FG} \left\{ 1 + 2\frac{1-(F+G)^{2N}}{[1-(F+G)](F+G)^{2N}} \right\} \cdot \frac{\sin[(2N+1)y]}{\sin y} \quad (82)$$

$$= 1.06078 \quad (83)$$

$$\sigma_3 \equiv 2\int_0^{\frac{\pi}{2}} dx \int_0^{\frac{\pi}{2}} dy \frac{F \cos^2 x}{G} \left\{ 1 + 2\frac{1-(F+G)^{2N}}{[1-(F+G)](F+G)^{2N}} \right\} \cdot \frac{\sin[(2N+1)x]}{\sin x} \cdot \frac{\sin[(2N+1)y]}{\sin y} \quad (84)$$

$$= 3.14570 \quad (85)$$

$$\sigma_4 \equiv 2\int_0^{\frac{\pi}{2}} dx \int_0^{\frac{\pi}{2}} dy \frac{\sin^2 x \sin^2 y}{F} \cdot \frac{\sin[(2N+1)x]}{\sin x} \cdot \frac{\sin[(2N+1)y]}{\sin y} \cdot [G-F] \quad (86)$$

$$= 4.24389 \times 10^{-2} \quad (87)$$

where,

$$F = F(x,y) \equiv \sqrt{\sin^2 x + \sin^2 y} \quad (88)$$

$$G = G(x,y) \equiv \sqrt{1 + \sin^2 x + \sin^2 y} \quad (89)$$

The factor of two included in front of each of the above integrals accounts for the dipole fields on the opposite side of the screen.

The above integrals were evaluated for $N = 1$, representing a 3×3 dipole array, which includes apertures at n and its eight nearest neighbors n'. In evaluating the above double integrals Simpson's rule was employed using double precision, and the integration subinterval size was successively reduced by a factor of three until the integration converged to within a fractional error of $.001$.

The corrected electric and magnetic currents are then given by,

$$K_x = \frac{\alpha_m}{\Delta}\left(\frac{\partial h_x}{\partial \tau} - (\frac{\partial h_{dx}}{\partial \tau})^{FDTD} + (\frac{\partial h_{dx}}{\partial \tau})^{ANAL}\right) \tag{90}$$

$$K_y = \frac{\alpha_m}{\Delta}\left(\frac{\partial h_y}{\partial \tau} - (\frac{\partial h_{dy}}{\partial \tau})^{FDTD} + (\frac{\partial h_{dy}}{\partial \tau})^{ANAL}\right) \tag{91}$$

$$\eta I_z = -\frac{\alpha_e}{\Delta}\left(\frac{\partial e_z}{\partial \tau} - (\frac{\partial e_{dz}}{\partial \tau})^{FDTD} + (\frac{\partial e_{dz}}{\partial \tau})^{ANAL}\right) \tag{92}$$

Substituting Equations (73)–(75) and (77)–(79) into the above and solving for the corrected currents gives the final equations for the corrected currents, which can be written,

$$\begin{aligned} K_x^p = &+ \alpha_2(\frac{a}{\Delta})^3(\eta\tilde{I}_z^p - \eta\tilde{I}_z^{p-1}) + [1 - \alpha_4(\frac{a}{\Delta})^3]\tilde{K}_x^p \\ &+ \alpha_5(\frac{a}{\Delta})^3\tilde{K}_y^p \end{aligned} \tag{93}$$

$$\begin{aligned} K_y^p = &- \alpha_2(\frac{a}{\Delta})^3(\eta\tilde{I}_z^p - \eta\tilde{I}_z^{p-1}) + \alpha_5(\frac{a}{\Delta})^3\tilde{K}_x^p \\ &+ [1 - \alpha_4(\frac{a}{\Delta})^3]\tilde{K}_y^p \end{aligned} \tag{94}$$

$$\eta I_z^p = [1 + \alpha_1(\frac{a}{\Delta})^3]\eta\tilde{I}_z^p + \alpha_3(\frac{a}{\Delta})^3(\tilde{K}_x^p - \tilde{K}_x^{p-1}) \tag{95}$$

where $K_x^p = K_x^p(l,m,n)$, $K_y^p = K_y^p(l,m,n)$ and $I_z^p = I_z^p(l,m,n)$ for an aperture at cell (l,m,n), and where,

$$\alpha_1 \equiv \frac{8\gamma_e}{\pi^2}(\sigma_1 + 2\sigma_2) \tag{96}$$

$$\alpha_2 \equiv \frac{2\gamma_m\sigma_1}{\pi^2}(\frac{\Delta}{\Delta\tau}) \tag{97}$$

$$\alpha_3 \equiv \frac{4\gamma_e\sigma_2}{\pi^2}(\frac{\Delta}{\Delta\tau}) \tag{98}$$

$$\alpha_4 \equiv \frac{8\gamma_m}{\pi^2}(\sigma_3 - \sigma_0) \tag{99}$$

$$\alpha_5 \equiv \frac{8\gamma_m\sigma_4}{\pi^2} \tag{100}$$

These equations are identical with those for the isolated aperture except that the constants α_n are different. In the next section the above equations are evaluated.

5. Evaluation for Closely-Spaced Apertures

The geometry we are considering is given in Figure 1. We have a plane wave incident on a perfectly conducting, infinitely thin perforated screen, where the perforations are in the form of either a 5×5 square array of apertures with spacing 2Δ, or an 11×11 square array of apertures with spacing Δ. The transmitted power without any correction for the 5×5 array is shown in Figure 4, where the transmitted power is divided by the analytical (dipole approximation) transmitted power. The plane wave excitation is incident normal to the screen with the electric field polarized in the y direction. Two sources of error are evident as in the isolated aperture case, the first depending on a/Δ, and the second on frequency, and the former error, as mentioned above, is twice that of the isolated aperture case presented in [1], owing to the error contributed by the dipoles on the transmission side of the screen.

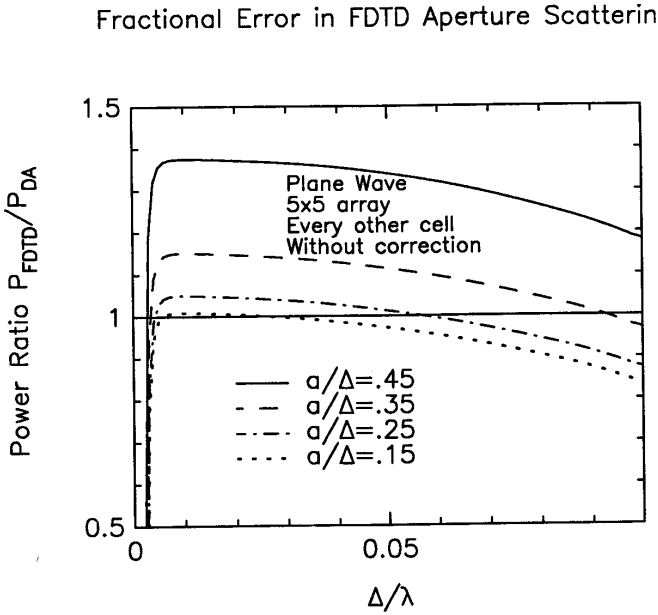

Figure 4. Transmitted power through 5×5 array of circular apertures without correction. Aperture in every other cell.

The deviation in power at the extreme low end of the band is due to the failure of the absorbing boundary conditions at low frequencies. If the equations given in [1] for an isolated aperture are used, modified so as to include sources on both sides of the screen, the transmitted power is as given in Figure 5.

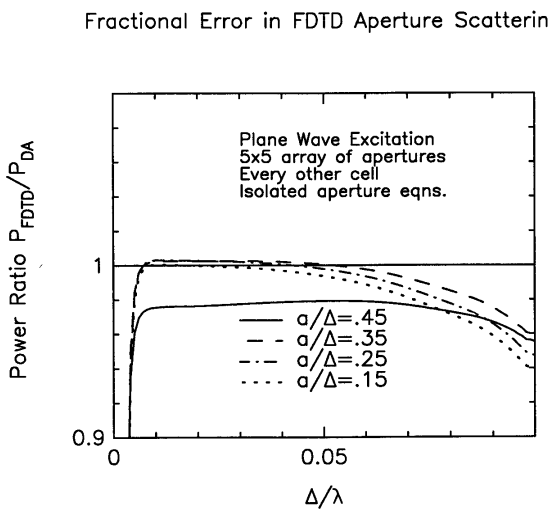

Figure 5. Transmitted power through 5×5 array of circular apertures. Aperture in every other cell. Isolated aperture correction.

It is evident that for the 5×5 array, where the spacing between apertures is 2Δ, the isolated aperture correction removes the a/Δ dependent error. Hence for this case the correction for the FDTD dipole fields is not necessary. The remaining frequency dependent error is discussed below. Results for the 11×11 array without correction are given in Figure 6. The error without correction for the 11×11 array is less than that for the 5×5 array. The reason for this is that the error in the dipole fields cancels a part of the error resulting from the dipole self-field. If we attempt to use the isolated aperture equations for the closely-spaced aperture array we see from Figure 7 that the error is over corrected, which is expected since we have already observed that the error in the dipole fields cancels part of the error resulting from the dipole self-field. Here the correction to the FDTD dipole fields is necessary. Applying the nearest-neighbors correction gives the transmitted power shown in Figure 8 . It is evident that the nearest-neighbor correc-

tion, to lowest order in frequency, is sufficient to correct for the error in the dipole fields. Figure 9 shows the transmitted power for non-normal incidence using the nearest-neighbor dipole field correction.

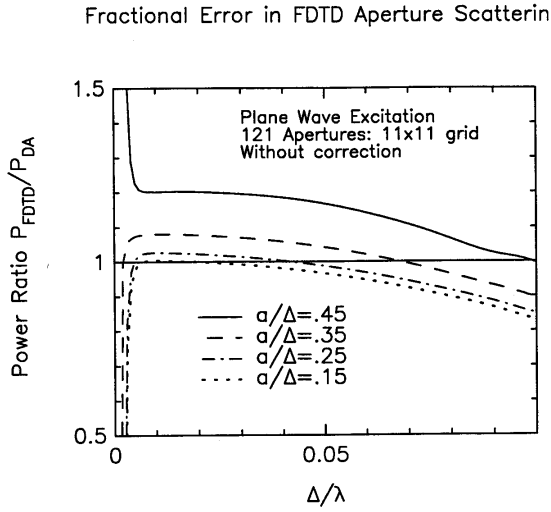

Figure 6. Transmitted power through 11×11 array of circular apertures without correction. Aperture in every cell.

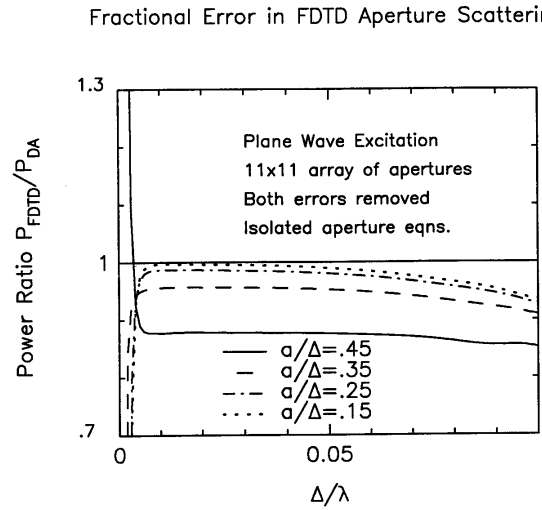

Figure 7. Transmitted power through 11×11 array of circular apertures with isolated aperture correction. Aperture in every cell.

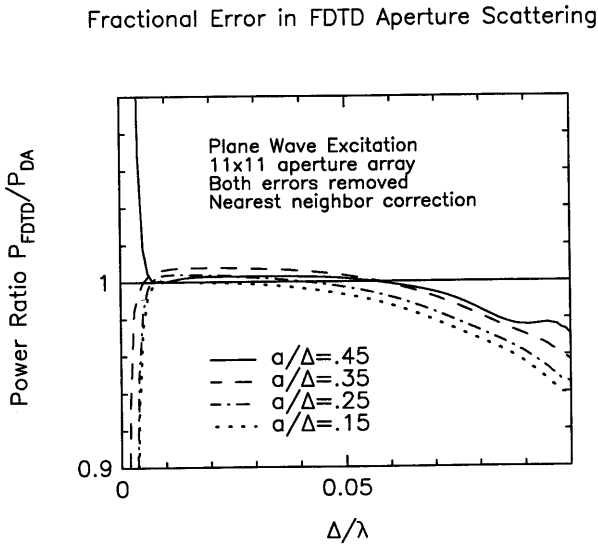

Figure 8. Transmitted power through 11×11 array of circular apertures with nearest-neighbors correction. Aperture in every cell.

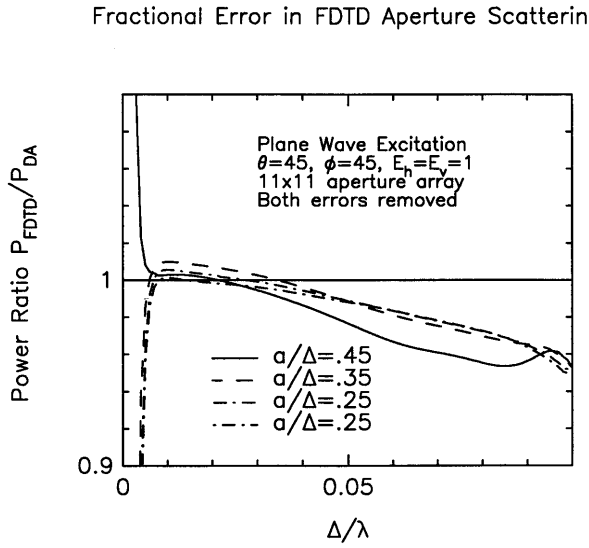

Figure 9. Transmitted power through 11×11 array of circular apertures for non-normal incidence using the nearest-neighbor dipole field correction. The incident field wave vector is given by the spherical coordinates $\theta = 45°$, $\phi = 45°$, and the electric field polarization is rotated $45°$ from the plane of incidence .

The incident field wave vector is given by the spherical coordinates $\theta = 45°$, $\phi = 45°$, and the electric field polarization is rotated $45°$ from the plane of incidence. The error for this case is not substantially different from that for normal incidence. Figure 10 shows the transmitted power for a dipole radiating behind the screen at a distance of 8 grid cells. The error for dipole excitation is nearly the same as that for plane wave excitation except at the low frequency band edge, where the discrepancy is due to reflections of the dipole fields from the absorbing boundary conditions.

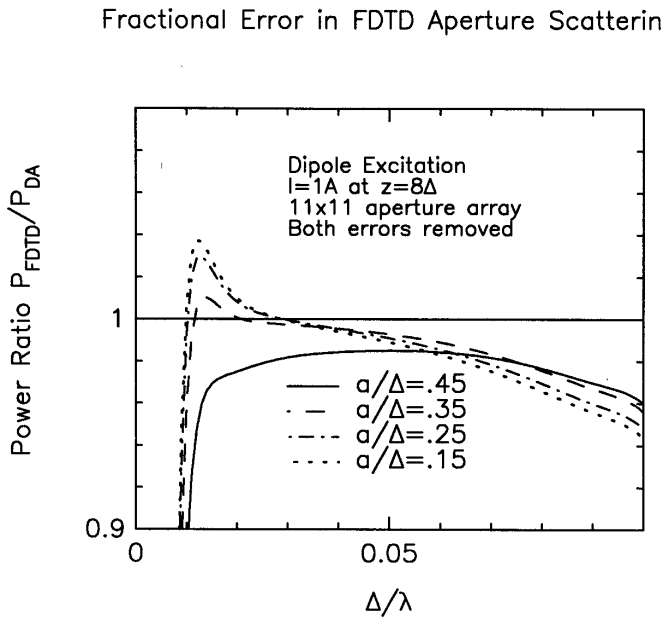

Figure 10. Transmitted power through 11×11 array of circular apertures using nearest-neighbors correction for a dipole radiating behind the screen at a distance of 8 grid cells.

The remaining frequency-dependent error evident in Figures 5–10 is due to the displacement of the dipoles a half grid cell from the perfect conductor. For a single dipole, such as used in the isolated aperture formulation, this error is canceled to a large extent by the error resulting from the discretization of time and space [1]. For an array of dipoles of equal or nearly equal amplitude and phase, however, this dipole displacement error is much larger. Figure 11 shows the error due to displacing an 11×11 array of dipoles a grid cell from

the image dipoles. Three curves are compared. The first curve shows the numerical FDTD results for an array of equally excited apertures for which the aperture radius is is small enough ($a/\Delta = 0.15$) so that aperture interaction is negligible, and hence the magnetic currents representing the apertures are nearly equal. The power radiated by an array of equal amplitude and phase magnetic currents in FDTD can also be calculated analytically. For a $(2N_x + 1) \times (2N_y + 1)$ array of dipoles displaced a half grid cell from a perfect conductor, the FDTD radiated power is given by,

$$P_{FDTD} = \frac{|qK_0\Delta|^2}{8\pi^2\eta} \cos(\frac{k\Delta\tau}{2}) \int_0^1 du \int_0^{2\pi} d\phi \frac{u}{\sqrt{1-u^2}} F(u, \phi; q\Delta/2) \tag{101}$$

$$= \frac{|qK_0\Delta|^2}{8\pi^2\eta} \cos(\frac{k\Delta\tau}{2}) \Big\{ 2\pi \sqrt{1 - (\frac{q\Delta}{2})^2} (2N_x + 1)^2 (2N_y + 1)^2 + \int_0^1 du \int_0^{2\pi} d\phi \sqrt{1-u^2} \frac{d}{du} F(u, \phi; q\Delta/2) \Big\} \tag{102}$$

$$F(u, \phi; q\Delta/2) \equiv \frac{\sqrt{1 - (\frac{q\Delta}{2})^2(1-u^2)}[1 - u^2\cos^2\phi](XY)^2}{\sqrt{1 - (\frac{q\Delta}{2})^2 u^2 + (\frac{q\Delta}{2})^4 u^4 \sin^2\phi\cos^2\phi}} \tag{103}$$

$$X \equiv \frac{\sin[(2N_x + 1)\sin^{-1}((\frac{q\Delta}{2})u\cos\phi)]}{(\frac{q\Delta}{2})u\cos\phi} \tag{104}$$

$$Y \equiv \frac{\sin[(2N_y + 1)\sin^{-1}((\frac{q\Delta}{2})u\sin\phi)]}{(\frac{q\Delta}{2})u\sin\phi} \tag{105}$$

$$q \equiv (\frac{2}{\Delta\tau}) \sin(\frac{k\Delta\tau}{2}) \tag{106}$$

This equation follows directly from the analytical solution to dipole radiation in FDTD presented in [1]. The second curve shows the analytically derived FDTD radiated power, which can be computed by numerically evaluating the above double integral. The third curve shows the corresponding continuum radiated power. The numerically computed and analytically derived FDTD radiated power are nearly equal. As for the isolated dipole, the FDTD radiated power for the dipole array is

higher than the continuum radiated power. The frequency-dependent error observed here is not due to a local inaccuracy, but results from the global interaction of the apertures. Hence this error cannot be corrected for as previously done [1] for the frequency-dependent error in the isolated aperture formulation.

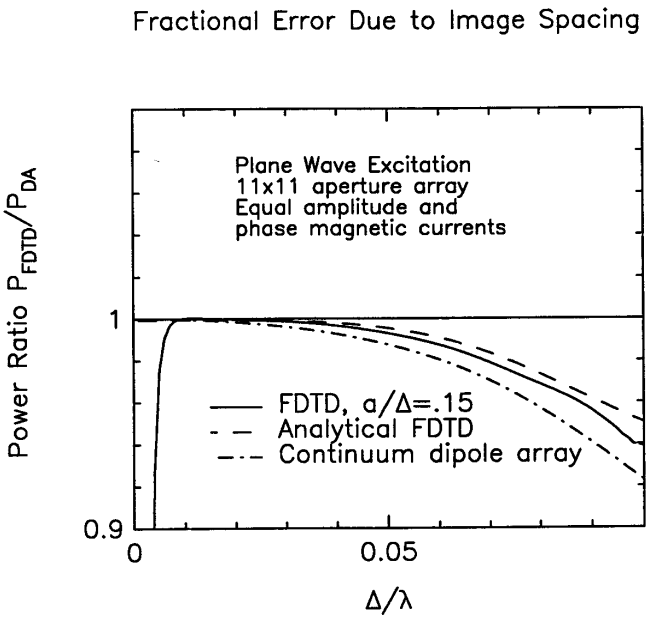

Figure 11. Fractional error in transmitted power through an 11×11 array of circular apertures due to the displacement of the primary and image dipoles by one grid cell.

6. Conclusions

The method previously presented for modeling an isolated small aperture using the FDTD technique [1] accurately models apertures which are spaced at least two grid cells apart. For closely spaced apertures, however, the isolated aperture formulation overcorrects the currents, and this is due to errors in the FDTD dipole fields. These errors can be accurately subtracted out by analytically subtracting out the FDTD dipole fields from neighboring apertures, and adding back in the correct fields. The method presented above, based on this approach,

models the dipole approximation to dense aperture arrays with an error of only a few percent.

Acknowledgment

This work was supported by the Office of Naval Research Grant N00014-92-J-4098, the Digital Equipment Corporation, and Joint Service Electronics Program under Contract DAAL03-92-C-0001.

References

1. Oates, J. H., R. T. Shin, and M. J. Tsuk, "Small aperture modeling for EMI applications using the FDTD technique," *JEMWA,* Vol. 9, No. 1/2, 37–69, 1995.
2. Rahmat-Samii, Y., and R. Mittra, "Electromagnetic coupling through small apertures in a conducting screen," *IEEE Trans. Anten. and Prop.,* Vol. AP-25, No. 2, 180–187, Mar. 1977.
3. Jan, I. C., R. F. Harrington, and J. R. Mautz, "Aperture admittance of a rectangular aperture and its use," *IEEE Trans. Anten. and Prop.,* Vol. 39, No. 3, 423–425, Mar. 1991.
4. Butler, C. M., "A formulation of the finite-length narrow slot or strip equation," *IEEE Trans. Anten. and Prop.,* Vol. AP-30, No. 6, 1254–1257, Nov. 1982.
5. Butler, C. M., and K. R. Umashankar, "Electromagnetic penetration through an aperture in an infinite, planar screen separating two half spaces of different electromagnetic properties," *Radio Science,* Vol. 11, No. 7, 611–619, July 1976.
6. Butler, C. M., and D. R. Wiltron, "General analysis of narrow strips and slots," *IEEE Trans. Anten. and Prop.,* Vol. AP-28, No. 1, 42–48, Jan. 1980.
7. Butler, C. M., Y. Rahmat-Samii, and R. Mittra, "Electromagnetic penetration through apertures in conducting surfaces," *IEEE Trans. Anten. and Prop.,* Vol. AP-26, No. 1, 82–93, Jan. 1978.
8. Gilbert, J., and R. Holland, "Implementation of the thin-slot formalism in the finite-difference EMP code THREDII," *IEEE Trans. Nuc. Sci.,* Vol. NS-28, No. 6, 4269–4274, Dec. 1981.
9. Holland, R., and L. Simpson, "Finite-difference analysis of EMP coupling to thin struts and wires," *IEEE Trans. Elect. Compat.,* Vol. EMC-23, No. 2, 88–97, May 1981.

10. Turner, C. D., and L. D. Bacon, "Evaluation of a thin-slot formalism for finite-difference time-domain electromagnetic codes," *IEEE Trans. Elect. Compat.,* Vol. 30, No. 4, 523–528, Nov. 1988.
11. Demarest, K. R., "A finite difference-time domain technique for modeling narrow apertures in conducting scatterers," *IEEE Trans. Anten. and Prop.,* Vol. AP-35, No. 7, 826–831, July 1987.
12. Reed, E. K., and C. M. Butler, "Time-domain electromagnetic penetration through arbitrarily shaped narrow slots in conducting screens," *IEEE Trans. Elect. Compat.,* Vol. 34, No. 3, 161–172, Aug. 1992.
13. Warne, L. K., and K. C. Chen, "Slot apertures having depth and losses described by local transmission line theory," *IEEE Trans. Elect. Compat.,* Vol. 32, No. 3, 185–196, Aug. 1990.
14. Warne, L. K., and K. C. Chen, "Relation between equivalent antenna radius and transverse line dipole moments of a narrow slot aperture having depth," *IEEE Trans. Elect. Compat.,* Vol . 30, No. 3, 364–370, Aug. 1988.
15. Warne, L. K., and K. C. Chen, "A simple transmission line model for narrow slot apertures having depth," *IEEE Trans. Elect. Compat.,* Vol. 34, No. 3, 185–196, Aug. 1992.
16. Jin, J. M., and J. L. Volakis, "TE scattering by an inhomogeneously filled aperture in a thick conducting plane," *IEEE Trans. Anten. and Prop.,* Vol. 38, No. 8, 1280–1286, July 1987.
17. Taflove, A., and J. L. Volakis, "Review of the formulation and application of the finite-difference time-domain method for numerical modeling of electromagnetic wave interactions with arbitrary structures," *Wave Motion,* Vol. 10, 547–582, Dec. 1988.
18. Archambeault, B., "EMI modeling of air vents and slots in shielded cabinets," *IEEE International EMC Symposium,* Anaheim, CA, Aug. 17–21, 1992.
19. Bethe, H. A., "Theory of diffraction by small holes," *Phys. Rev.,* Vol. 66, 163–182, Oct. 1944.
20. Collin, R. E., *Field Theory of Guided Waves*, New York, McGraw-Hill, 1960.
21. Eggimann, W. H., "Higher-order evaluation of electromagnetic diffraction by circular disks," *IEEE Trans. Microwave Theory and Tech.,* 408–418, Sept. 1961.

22. Lord Rayleigh, "On the incidence of aerial and electric waves on obstacles in the form of ellipsoids or elliptic cylinders, on the passage of electric waves through a circular aperture in a conducting screen," *Phil. Mag.,* Vol. 44, p. 28, 1987.
23. Collin, R. E., and W. H. Eggimann, "Dynamic interaction fields in a two-dimensional lattice," *IRE Trans. Microwave Theory Tech.,* Vol. MTT-9, 110–115, March 1961.
24. Kieburtz, R. B., and A. Ishimaru, "Aperture fields of an array of rectangular apertures," *IRE Trans. Antennas Propagat.,* Vol. AP-10, 663–671, Nov. 1962.
25. Chen, C. C., "Transmission through a conducting screen perforated periodically with apertures," *IEEE Trans. Microwave Theory Tech.,* Vol. MTT-18, Sept. 1970.
26. Chen, C. C., "Transmission of microwaves through perforated flat plates of finite thickness," *IEEE Trans. Microwave Theory Tech.,* Vol. MTT-21, 1–6, Jan. 1973.
27. Collin, R. E., *Foundations for Microwave Engineering*, New York, McGraw-Hill, 1966.